Available online at www.sciencedirect.com

SCIENCE DIRECT

International Journal of Mass Spectrometry 253 (2006) 122–129

www.elsevier.com/locate/ijms

Absolute partial cross sections and kinetic energy analysis for the electron impact ionization of propene

S. Feil, A. Bacher, K. Gluch[1], S. Matt-Leubner, P. Scheier, T.D. Märk[*,2]

Institut für Ionenphysik und Angewandte Physik, Leopold Franzens Universität Innsbruck, Technikerstr. 25, A-6020 Innsbruck, Austria

Received 28 February 2006; received in revised form 18 April 2006; accepted 18 April 2006

Abstract

We present absolute partial electron impact ionization cross sections for propene in the electron energy range between threshold and 1000 eV measured with a two sector field double focussing mass spectrometer. Ion beam profiles have been measured at all electron energies by applying a deflection field method. In combination with a three-dimensional ion trajectory simulation of ions produced in the ion source ion kinetic energy distribution functions and discrimination factors can be derived form these data. Multiplication of these discrimination factors with the measured ion signals leads to relative partial cross sections. Normalization of the sum of the relative partial cross sections to an absolute total cross section gives absolute partial cross section values. The initial kinetic energy distributions of several fragment ions show the presence of two or more contributions exhibiting different electron energy dependencies. Differential cross sections with respect to initial kinetic energy of the ions are given and related to specific ion production channels. The high energetic parts of the initial kinetic energy distributions are assigned to the Coulomb explosion of doubly charged short-lived intermediates. The reaction $C_3H_5^{2+} \rightarrow C_2H_2^+ + CH_3^+$ has been studied quantitatively in the ion source, the first field free region and the second field free region of the two sector field mass spectrometer yielding a measured mean kinetic energy release of 4.99 ± 0.5 eV, 4.85 ± 0.5 eV and 5.5 ± 0.5 eV, respectively in good agreement with a theoretical estimation.

Keywords: Mass spectrometry; Absolute cross sections; Electron impact ionization; Propene; Ion kinetic energy

1. Introduction

The investigation of small hydrocarbons has recently regained importance in the field of molecular physics as these molecules are considered to be prototypes of polyatomic molecules. They are important constituents in planetary and cometary atmospheres and in plasmas [1–4], especially in fusion plasmas where they play a key role in the characterization of the edge region of magnetically confined hydrogen plasmas. Almost all modern fusion devices contain carbon as one of the plasma facing materials. The composition of the hydrocarbons entering the plasma may cover a wide range from CH up to C_3H_8 [5]. The release of more complex hydrocarbons from the plasma walls such as C_2H_6 and C_3H_6 becomes increasingly significant as the impact energy of plasma ions impinging on the surface decreases [6,7].

Reliable absolute total and also partial ionization cross sections are needed to understand the behavior of these plasmas. For instance, different reaction pathways can lead to the same specific product ion. In the case of propene the fragment ion $C_2H_2^+$ can be formed via a single dissociation process,

$$C_3H_6 + e^- \rightarrow C_2H_2^+ + 2e^- + \text{neutrals} \tag{1}$$

as well as by the prompt or delayed Coulomb explosion of a doubly charged precursor.

$$C_3H_6 + e^- \rightarrow C_3H_5^{2+} + H + 3e^- \tag{2}$$

$$C_3H_5^{2+} \rightarrow C_2H_2^+ + CH_3^+ \tag{2a}$$

These $C_2H_2^+$ ions that are produced have the same mass per charge ratio and structure, but they differ substantially in their kinetic energy. This information is important since the interaction of an ion with its environment is strongly dependent on its

---

[*] Corresponding author. Tel.: +43 512 507 6240; fax: +43 512 507 2932.
E-mail address: Tilmann.Maerk@uibk.ac.at (T.D. Märk).

[1] Permanent address: Department of Physics, University Marie Curie Sklodowskiej, Lublin, Poland.

[2] Also adjunct professor at Department of Experimental Physics, Comenius University, SK-84248 Bratislava, Slovak Republic.

1387-3806/$ – see front matter © 2006 Elsevier B.V. All rights reserved.
doi:10.1016/j.ijms.2006.04.006

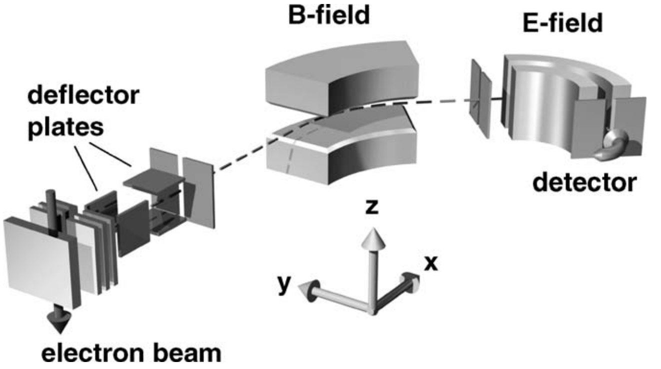

Fig. 1. Schematic view of the experimental setup. The two pairs of parallel plates for deflection of the ion beam perpendicularly to the beam direction are designated as deflector plates.

kinetic energy. Furthermore, in the case of plasma sheath modelling, data about the kinetic energy of hydrocarbons that are formed via electron molecule reactions are needed in order to estimate the energy balance in the plasma edge region. An analysis of ion yield profiles (*z* profiles, see below and [8]) recently established in our lab enables us to distinguish between the processes that lead to the same product ion.

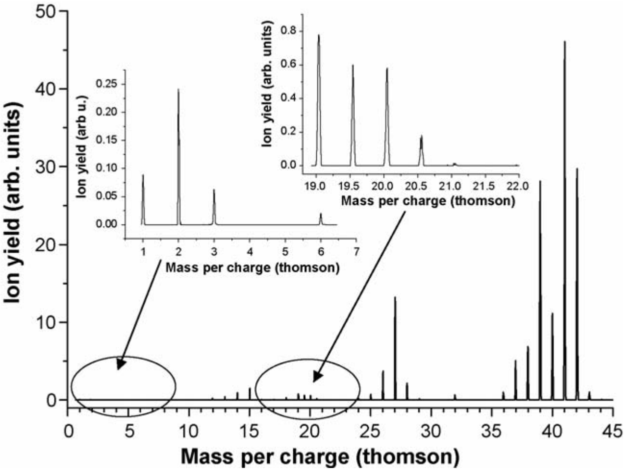

Fig. 2. Mass spectrum of propene, recorded at an electron energy of 100 eV and an electron current of 10 μA. Note that the spectrum is corrected for the residual background but not for discrimination effects due to the apparatus.

In 1994 Nishimura and Tawara [9] measured total electron impact ionization cross sections for various simple hydrocarbon molecules from threshold up to 3 keV. In the case of C_3H_6, they reported slightly different total ionization cross sections

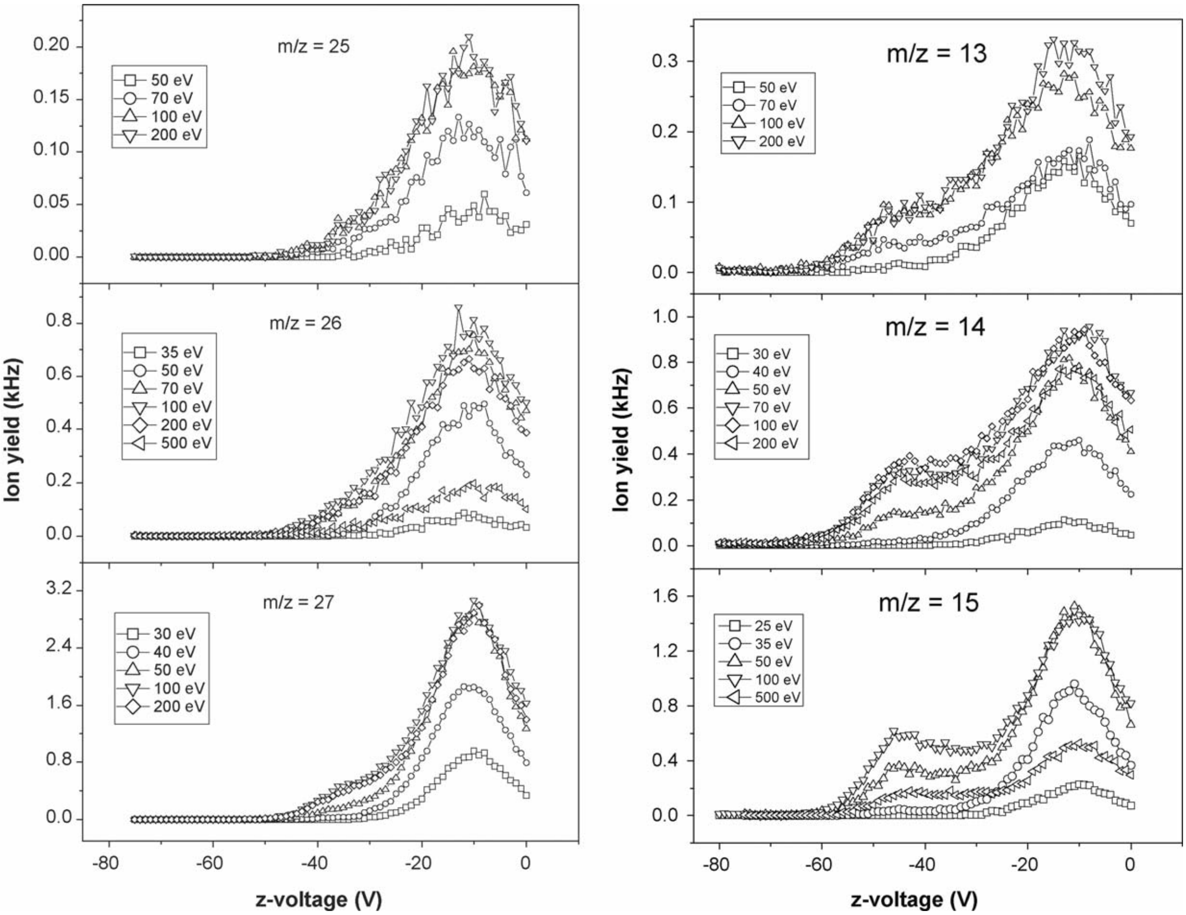

Fig. 3. Ion beam profiles (*z* profiles) of the fragments with a mass to charge ratio of 13–15 thomson and 25–27 thomson. The ion yield was measured as a function of the voltage on the *z*-deflector plates. Different line styles and symbols designate different electron energies. Note that the profile for the fragment ions with the mass to charge ratio of 13–15 thomson are clearly bimodal.

for isomeric cyclopropane and propene. Deutsch et al. [6] using the DM formalism calculated absolute total electron impact ionization cross sections for the two C_3H_6 isomers cyclopropane ($-H_2C-CH_2-CH_2-$) and propene ($H_2C=CH-CH_3$). The agreement between the calculated cross sections and the experimentally determined cross sections was excellent in terms of the absolute magnitude for impact energies below 100 eV and satisfactory for higher impact energies. However, the DM calculation did not reproduce the slight isomer effect that was found in the experimental data. The measured ionization cross section for propene was found to be larger by a few percent than the cross section for cyclopropane.

Here we determine absolute partial electron impact ionization cross sections and also derive the dependence of the partial cross sections on the initial kinetic energy of the fragment ions. When Wang and Vidal [10] in 2002 investigated electron impact on propane (C_3H_8), they observed a large variety of multiply charged ions. For instance, they could see a doubly charged fragment with a mass of 41 Da ($C_3H_5{}^{2+}$) that decays into the fragments $C_2H_2{}^+$ and $CH_3{}^+$. We can see the same reaction via electron impact on neutral C_3H_6. Techniques used here for investigating reactions such as $C_3H_5{}^{2+} \rightarrow C_2H_2{}^+ + CH_3{}^+$ are: (i) a technique for the measurement of ion yield profiles (z profiles), (ii) the mass analyzed kinetic energy (MIKE) scan technique and (iii) the high voltage (HV)-scan technique.

2. Experimental

The apparatus used in this study is a double focusing two-sector-field mass spectrometer of reversed geometry with a Nier-type electron-impact ion source and has been described in detail in earlier publications [11,12]. Fig. 1 shows the experimental setup schematically. A stagnant target gas is crossed by a well-characterized magnetically collimated electron beam with a FWHM energy spread of ∼0.5 eV. Product ions are extracted from the ion source either by a weak penetrating electric field (typically 50 V/m) or by a strong homogeneous electric field (3 kV/m) generated with the lenses that are part of the front and back side of the interaction region of the electron beam with the neutral molecules. They are then accelerated to 3 kV before entering the analyzing part of the mass spectrometer through a narrow entrance slit, the ions pass two pairs of perpendicular deflection plates that allow the ion beam to be steered in the y- and z-direction. These deflection plates are used in cross section measurements to sweep the extracted ion beam across the entrance slit [13] and to integrate the detected ion signal. After passing through a magnetic sector field followed by an electric sector field, the ions are detected by a secondary electron multiplier operated in the pulse counting mode. The combined action of the two sector fields in a double focusing mass spectrometer results in a focusing of the ions within the plane of the instrument

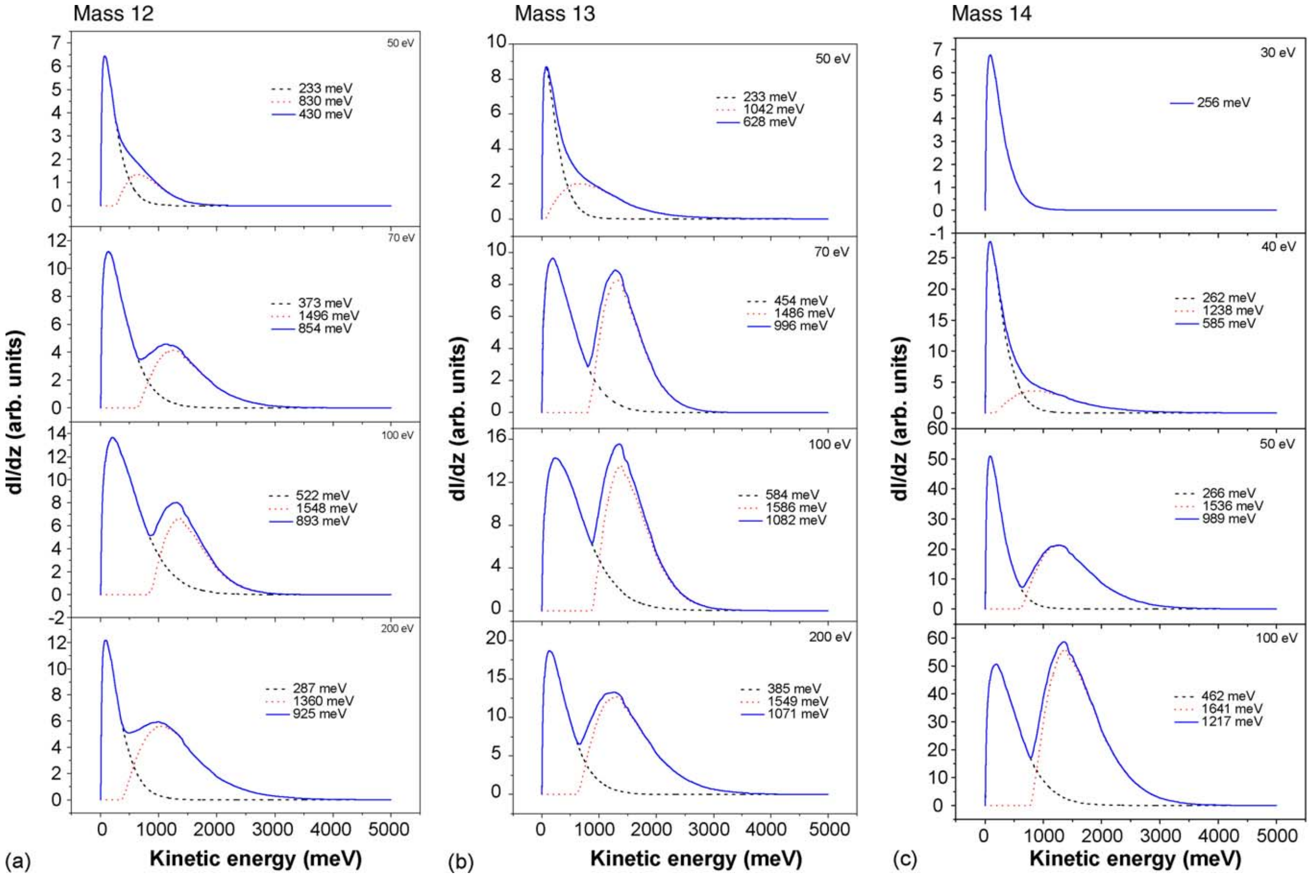

Fig. 4. (a–f) Kinetic energy distribution functions (full line) for the fragments with m/z 12–15 and 25–27 thomson. Almost all of the distribution functions (shown here for electron energies above 30 eV) are of bimodal shape corresponding to two different groups of ions (low energy ions designated by the dashed and high energy ions designated by the dotted line). Also the corresponding average kinetic energies are given in meV for the total curve and the two separated curves.

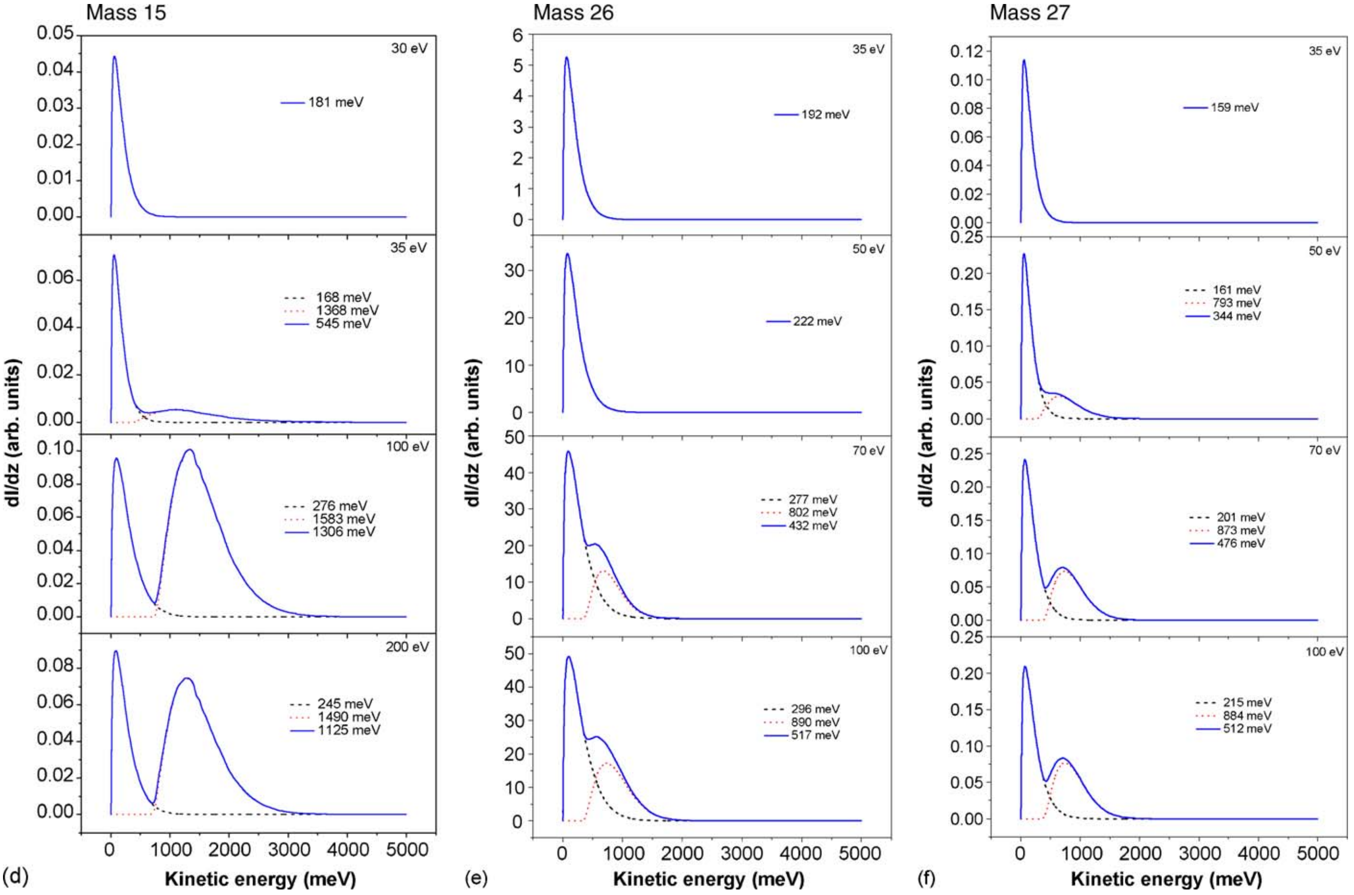

Fig. 4. (*Continued*).

which corrects for the angular and spatial spreads of the starting points of the ions and for small variations in the kinetic energy. However, the only way to compensate a velocity component outside of the plane of the instrument (*z*-direction, see Fig. 1) is a corrective action with the so called *z*-deflector plates right after the ion source. The ion yield, measured as a function of the *z*-deflection voltage, allows the determination of the kinetic energy distribution for a given fragment ion [11,14]. However, the weak penetrating field that is normally applied cannot extract fragment ions that have initial kinetic energies in the *z*-direction larger than 100 meV [15]. With the repeller (located in the back of the ion source) and the first lenses that form the front of the interaction region (of the electrons and the neutral molecules), it is possible to generate a strong homogeneous electric field that is able to extract ions with initial kinetic energies up to several eV into the *z*-direction. This mode of operation has to be chosen to determine the kinetic energy distribution of swift fragment ions.

In the present case of propene, decay reactions of dications do not only occur in the ion source immediately after electron impact, but also occur in a metastable time regime. We use the high voltage (HV) scan technique for the measurement of metastable decay reactions of the kind

$$\mathrm{m}_1^{z_1+} \rightarrow \mathrm{m}_2^{z_2+} + \mathrm{m}_3^{z_3+} \qquad (3)$$

occurring in the first field free region (ff1) and the mass analyzed ion kinetic energy (MIKE) scan technique in the second field free region (ff2). Beynon and co-workers [16] have shown that the translational kinetic energy release T in the simple charge separation reaction (3) can be calculated from the corrected (i.e., for the width of the precursor ion peak) width of the metastable peaks ΔV and ΔE using the relations

$$T = \frac{z_1^2 m_2^2 U_0}{16 z_2 m_1 m_3}\left(\frac{\Delta U}{U_0}\right)^2 \qquad (4)$$

$$T = \frac{z_2^2 m_1^2 U_0}{16 z_1 m_2 m_3}\left(\frac{\Delta E}{E_0}\right)^2 \qquad (5)$$

where z_1 and m_1 are the charge state and mass of the precursor ion, z_2 and m_2 are the charge state and mass of the detected fragment ion, m_3 is the mass of the undetected fragment ion, U_0 is the acceleration voltage and E_0 is the sector field voltage required for the detection of the precursor ion.

3. Results and discussion

Fig. 2 presents a mass spectrum of propene that has been produced by the impact of electrons with a kinetic energy of 100 eV. The propene pressure has been set to 4×10^{-5} Pa and the electron current has been fixed to 10 μA. The spectrum is corrected for the residual background but not for discrimination effects that occur as a consequence of the initial kinetic energies of the fragment ions. Therefore the peak heights do not correlate with the cross section values at 100 eV. The most intense peak at a mass to charge ratio (*m*/*z*) of 41 thomson corresponds to the fragment $C_3H_5^+$. Two other groups of peaks can be observed around the mass to charge ratio of 15 thomson and 27 thomson (CH_3^+ and $C_2H_3^+$) with weaker peaks around the main signal corresponding to the C or C_2 core atoms, respectively with a different number of hydrogen atoms. Although the identification of doubly charged ions in mass spectra is sometimes challenging, it can be done easily here. Dications are unambiguously identified at half integer (*m*/*z*) ratios of 19.5 ($C_3H_3^{2+}$) and 20.5 ($C_3H_5^{2+}$) and the peaks in between at integer masses 19 and 20 are due to $C_3H_2^{2+}$ and $C_3H_4^{2+}$ since there is no possibility to produce singly-charged ions via electron impact on C_3H_6 in this mass range.

Fig. 3 shows ion beam profiles (*z* profiles) that have been measured after tuning the mass spectrometer to a specific mass to charge ratio and then sweeping the ion signal across the *z*-deflector-plates in the ion source. Maximum extraction conditions are used in the ion source in order to be able to detect ions with high initial kinetic energy. A straight-forward application of the ion deflection method yields a direct proportionality between the square of the deflection voltage in the *z*-direction and the kinetic energy of the ions in the laboratory system [11,17,18]. In order to elucidate the behaviour of the *z* profiles in more detail, we analyzed these beam profiles in a more quantitative way (for details see Ref. [15]). The initial ion kinetic energy distribution and the extraction efficiency (discrimination factor) from the ion source for a given product ion are determined by fitting measured ion beam *z* profiles with a superposition of simulated ion beam profiles. The position where these ions are formed is randomly taken within the volume that is covered by the electron beam. Thereby, ion loss to the walls of the ion source housing is included in the resulting *z* profiles of the ion beam. In contrast to earlier fitting methods the present technique of fitting a weighted superposition of 3D simulated *z* profiles to the experimental data allows the analysis of ion beam profiles of highly energetic fragment ions that are affected by the reduced ion extraction efficiency.

In general the kinetic energy of a given fragment ion consists of the initial thermal energy of the neutral propene molecule in the ion source (which is usually identical to the temperature of the neutral gas emanating from the gas nozzle) and any kinetic energy imparted to the fragment ion under study by the dissociative ionization process. For example, in the case of the fragment with mass to charge ratio of 15 thomson (see Fig. 3), there are two main contributions (one with high kinetic energy and one with low kinetic energy) that contribute to the profile. In order to determine the origin of the two contributions one has to identify the production pathways of the fragment with (*m*/*z*) 15 thomson. The fragment ion can be formed via a single ionization process, or, as also observed by Wang and Vidal [10], via Coulomb explosions of $C_3H_5^{2+}$ precursor ions. Wang and Vidal [10] have shown that electron impact on C_3H_8 forms doubly charged $C_3H_5^{2+}$. This dication then decays into $C_2H_2^+$ and CH_3^+. We can investigate the same reaction following electron impact on propene. That is why we see high energetic parts (which originate from Coulomb explosion) at (*m*/*z*) ratios 12–15 thomson and 25–27 thomson in the *z* profiles.

In Fig. 4a–f kinetic energy distribution functions are presented for the most prominent fragment ions. In all cases shown the distribution consists of two distributions (low and high kinetic energy part, see curves shown in Fig. 4 for the different electron energies). In general we find that by increasing the electron energy the mean kinetic energy of the distribution also increases. The high-energy contribution starts to grow until an electron energy of approximately 100 eV and decreases afterwards.

The discrimination effects of the different fragment ions (during extraction out of the ion source) can be deduced via analysis of the z profiles as discussed above and this allows one to correct the measured relative cross section curves. The final absolute cross section curves (Fig. 5) are obtained in the following way. Partial ion intensity curves are measured first and then they are corrected for discrimination effects. They are then summed up and normalized to the value at 100 eV electron energy of the total cross section curve obtained by Nishimura and Tawara [9] (see also [19,20] for the method). All the measured absolute partial cross sections are presented in Fig. 5, as far as we can

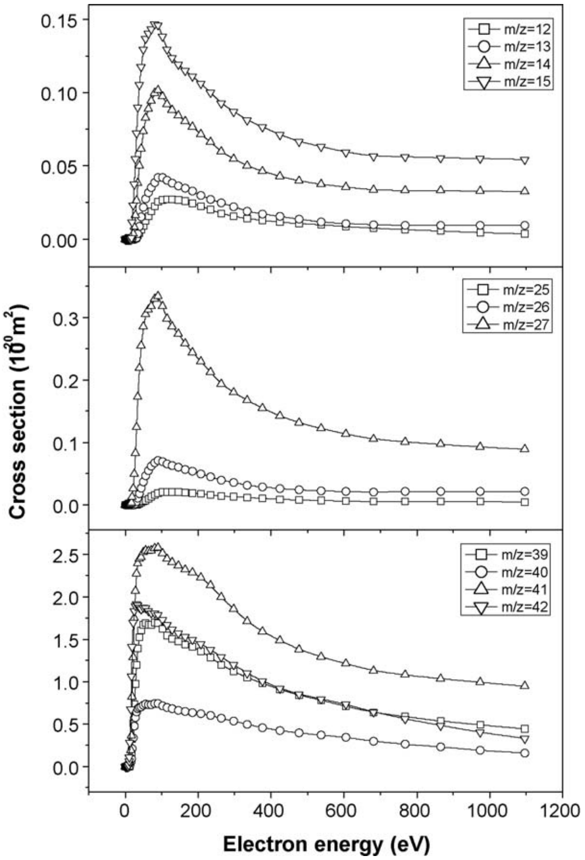

Fig. 5. Absolute partial cross sections for all fragments that are formed via electron impact of propene. The sum of the measured relative partial cross sections is calibrated to the total cross section value at 100 eV given by Nishimura and Tawara [9].

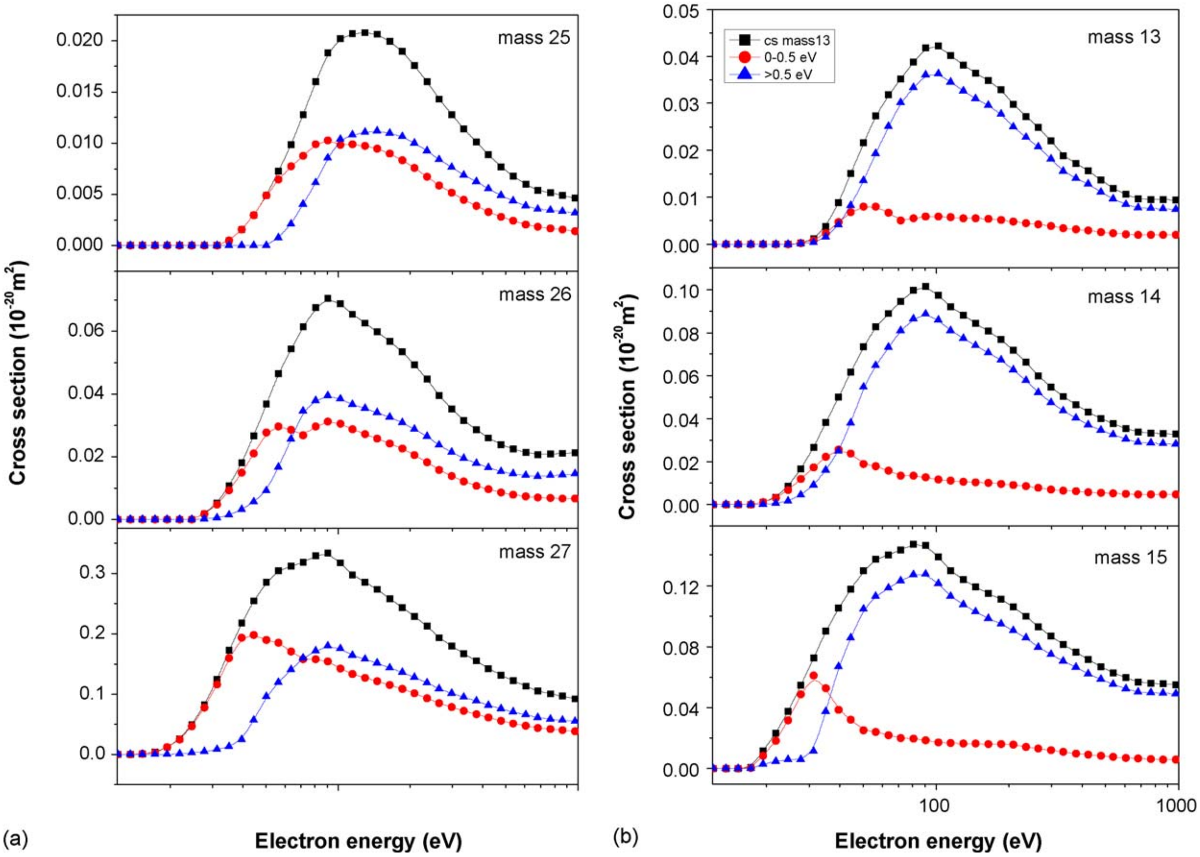

Fig. 6. (a and b) Absolute partial cross sections and absolute differential (with respect to their initial kinetic energy) cross sections corresponding to a low energy quasi thermal part (<0.5 eV) and to a high kinetic energy part (>0.5 eV).

tell these are the first experimental results for these partial cross sections reported in literature. The maximum cross section (i.e., for $m/z = 39$ thomson corresponding to $C_3H_3^+$) can be seen to have a value around 2.6×10^{-20} m^2.

Differential (with respect to the initial kinetic energy) partial cross sections for the formation of fragments with m/z ratios 25–27 and 13–15 thomson are shown in Fig. 6a and b. The general procedure for obtaining these differential cross sections has already been explained in [8,20]. In brief, we deduce the kinetic energy distribution function from the measured z-profile and then we divide the distribution function into two parts. The first part ranges from 0 to 0.5 eV and the second part from 0.55 to 10 eV. We define the probability of a specific ion with an energy in the low range with P_{I} and the probability of the high range with P_{II}. We repeat this for all electron energies and then get the probabilities P_{I} and P_{II} as a function of the electron energy. Finally, we multiply these functions with the cross section curves and obtain differential cross sections with respect to the initial kinetic energy of the ion as shown in Fig. 6.

In general, the analysis for masses 13–15 and 25–27 shows that the threshold for the cross section of the high energetic fragments is above the threshold for the formation of thermal ions. This indicates that the ions with high kinetic energy are predominantly formed by Coulomb explosion of the doubly charged species. Nevertheless, it should be mentioned here that such energetic fragment ions have also been detected from the population and fragmentation of highly excited "Rydberg" states of singly charge ions converging on the various doubly ionized states [21]. In effect such states are a dication core, which dissociates like a dication, plus a Rydberg electron which attaches to one of the fragments. The neutral fragment sometimes then autoionizes to yield a pair of monocations which actually result from the fragmentation of a singly charged state. The population of such states may well contribute somewhat to the yield of energetic fragment monocations, particularly near the double ionization threshold.

Moreover, it is interesting to note that the threshold for the fragment ions CH_3^+ and $C_2H_2^+$ with high initial kinetic energy is in both cases at around 30 eV. This indicates that these ions may be produced by the same reaction, i.e., $C_3H_5^{2+} \rightarrow C_2H_2^+ + CH_3^+$. To further elucidate this point we have investigated the stability of the dication ($C_3H_5^{2+}$) with help of the high voltage scan technique (Fig. 7) and the MIKE scan technique (Fig. 8). Eqs. (4) and (5) allow to deduce a mean kinetic energy release for the Coulomb explosion reaction of about $T = 5.5 \pm 0.5$ eV for the decay in ff2 (MIKE-scan) and 4.85 ± 0.5 eV for the decay in ff1 (HV-scan). These results are in good agreement with the estimation of this energy just by using Eq. (6) with R equal 2.8 Å (the distance between the charges; C=C bond 1.3 Å; C–C bond 1.5 Å) and assuming that the charges

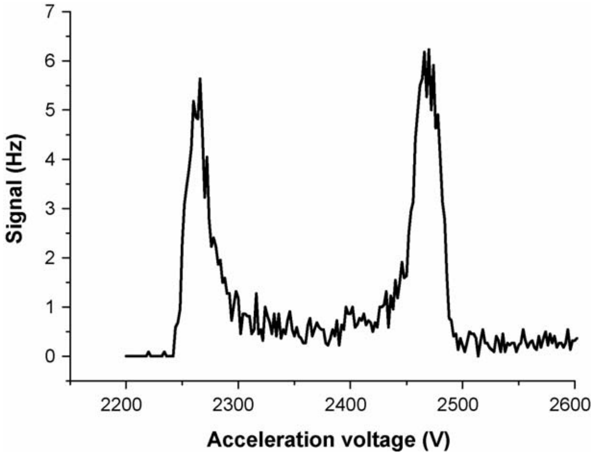

Fig. 7. HV-scan for the decay reaction $C_3H_5^{2+} \rightarrow C_2H_2^+ + CH_3^+$ in the first field free region.

are located at the C atoms at the ends of the chain [16,19].

$$T = \frac{14.39}{R} \rightarrow T = 5.14\,\text{eV} \tag{6}$$

Another way to obtain an estimation for this mean kinetic energy release for the Coulomb explosion of the $C_3H_5^{2+}$ is to calculate the energy release from the z profiles in the centre of mass system. For this one takes the maximum width of the *z*-profile shown in Fig. 3 and uses the proportionality between the square of the *z*-voltage and the corresponding kinetic energy (see [11]). For instance, the width of the fragment with mass to charge ratio of 15 thomson can be estimated from Fig. 3 to have a value of 60 V. This value corresponds to a kinetic energy of 2.94 ± 0.5 eV. A kinetic energy of 2.05 ± 0.5 eV is obtained for the fragment with mass to charge ratio of 26 thomson. The sum of these two kinetic energies, 4.99 ± 0.5 eV, agrees quite well with the mean kinetic energy that we have deduced with the help of the MIKE technique or the HV-scan technique.

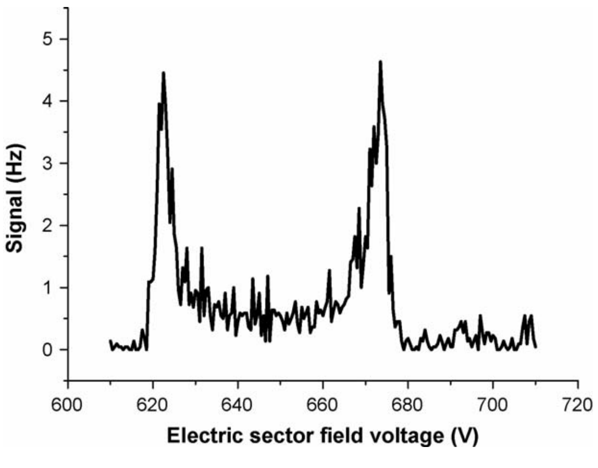

Fig. 8. MIKE-scan for the decay reaction $C_3H_5^{2+} \rightarrow C_2H_2^+ + CH_3^+$ in the second field free region.

4. Conclusions

In conclusion, the present measurements constitute the first experiment where a Coulomb explosion reaction therefore has been observed and quantitatively analyzed right after production of the precursor ion (leading to a prompt dissociation in the ion source) and at a later (metastable decay reaction) time in the field free regions. In both cases the full Coulomb energy is released into kinetic energy of the two fragment ions.

Finally it is quite remarkable that some of the graphs in Fig. 6a show a large difference in the appearance energy for the fragments with high (greater than 0.5 eV) and low (smaller than 0.5 eV) kinetic energy. For instance the fragment with a *m/z* ratio of 27 thomson is almost exclusively produced with low kinetic energy if one uses electrons with electron energy smaller than 35 eV. Therefore in some cases one can in principle produce ions with a specified kinetic energy just by tuning the energy of the electrons, accordingly.

Acknowledgements

This work was partly supported by the FWF, Wien, and the European Commission, Brussels (network program) and has been performed within the Association EURATOM-ÖAW. The content of the publication is the sole responsibility of its publishers and it does not necessarily represent the views of the EU Commission or its services.

References

[1] R.K. Janev (Ed.), Atomic and Molecular Processes in Fusion Edge Plasmas, Plenum, New York, 1995.

[2] M.C. McMaster, W.L. Hsu, M.E. Coltrin, D.S. Dandy, C. Fox, Diam. Relat. Mater. 4 (1995) 1000.

[3] H.W. Moos, J.T. Clark, Astrophys. J. 229 (1979) L107.

[4] T.C. Owen, J. Caldwel, A.R. Rivolo, V. Moore, A.L. Lane, C. Sagan, H. Hunt, C. Ponnamperuma, Astrophys. J. 236 (1987) L39.

[5] W.O. Hofer, E. Roth, Physical Process of interaction of fusion plasmas with solids, San Diego, 1996.

[6] H. Deutsch, K. Becker, R.K. Janev, M. Probst, T.D. Märk, J. Phys. B: At. Mol. Opt. Phys. 33 (2000) L865.

[7] J.W. Davies, A.A. Haasz, P.C. Stangeby, J. Nucl. Mater. 151–157 (1998) 234.

[8] K. Gluch, P. Scheier, W. Schustereder, T. Tepnual, L. Feketeova, C. Mair, S. Matt-Leubner, A. Stamatovic, T.D. Märk, Int. J. Mass Spec. 228 (2003) 307.

[9] H. Nishimura, H. Tawara, J. Phys. B: At. Mol. Opt. Phys. 27 (1994) 2063.

[10] P. Wang, C.R. Vidal, Chem. Phys. 280 (2002) 309.

[11] H.U. Poll, V. Grill, S. Matt, N. Abramzon, K. Becker, P. Scheier, T.D. Märk, Int. J. Mass Spectrom. Ion Proc. 177 (1998) 143.

[12] V. Grill, G. Walder, D. Margreiter, T. Rauth, H.U. Poll, P. Scheier, T.D. Märk, Z. Phys. D 25 (1993) 217.

[13] V. Grill, G. Walder, P. Scheier, M. Kurdel, T.D. Märk, Int. J. Mass Spectrom. Ion Proc. 129 (1993) 31.

[14] R. Taubert, Z. Naturforschg. 19a (1964) 484;
R. Fuchs, R. Taubert, Z. Naturforschg. 19a (1964) 494;
R. Taubert, Z. Naturforschg. 19a (1964) 911;
R. Fuchs, R. Taubert, Z. Naturforschg. 19a (1964) 1181.

[15] S. Feil, A. Bacher, M. Zangerl, W. Schustereder, K. Gluch, P. Scheier, Int. J. Mass Spectrom. 233 (2004) 325.

[16] R. Cooks, L.H. Beynon, R.M. Caprioli, G.R. Lester, Metastable Ions, Elsevier, Amsterdam, 1973.
[17] D.K. Sen Sharma, J.L. Franklin, Int. J. Mass Spec. Ion Phys. 13 (1974) 139.
[18] F.W. McLafferty, Mass Spectrometry of Organic Ions, Academic, New York.
[19] K. Gluch, J. Fedor, S. Matt-Leubner, O. Echt, A. Stamatovic, M. Probst, P. Scheier, T.D. Märk, J. Chem. Phys. 118 (2003) 3090.
[20] S. Feil, K. Gluch, S. Matt-Leubner, P. Scheier, T.D. Märk, J. Chem. Phys., 2006, in press.
[21] Y. Hikosaka, J.H.D. Eland, Chem. Phys. 299 (2004) 147.